JCI insight

RESEARCH ARTICLE

Wnt/β-catenin–activated Ewing sarcoma cells promote the angiogenic switch

Allegra G. Hawkins,[1] Elisabeth A. Pedersen,[2] Sydney Treichel,[1] Kelsey Temprine,[1] Colin Sperring,[1] Jay A. Read,[1] Brian Magnuson,[3] Rashmi Chugh,[3,4] and Elizabeth R. Lawlor[1,2,3]

[1]Department of Pediatrics, [2]Department of Pathology, [3]Rogel Cancer Center, and [4]Department of Internal Medicine, University of Michigan, Ann Arbor, Michigan, USA.

Wnt/β-catenin signaling is active in small subpopulations of Ewing sarcoma cells, and these cells display a more metastatic phenotype, in part due to antagonism of EWS-FLI1–dependent transcriptional activity. Importantly, these β-catenin–activated Ewing sarcoma cells also alter secretion of extracellular matrix (ECM) proteins. We thus hypothesized that, in addition to cell-autonomous mechanisms, Wnt/β-catenin–active tumor cells might contribute to disease progression by altering the tumor microenvironment (TME). Analysis of transcriptomic data from primary patient biopsies and from β-catenin–active versus –nonactive tumor cells identified angiogenic switch genes as being highly and reproducibly upregulated in the context of β-catenin activation. In addition, in silico and in vitro analyses, along with chorioallantoic membrane assays, demonstrated that β-catenin–activated Ewing cells secreted factors that promote angiogenesis. In particular, activation of canonical Wnt signaling leads Ewing sarcoma cells to upregulate expression and secretion of proangiogenic ECM proteins, collectively termed the angiomatrix. Significantly, our data show that induction of the angiomatrix by Wnt-responsive tumor cells is indirect and is mediated by TGF-β. Mechanistically, Wnt/β-catenin signaling antagonizes EWS-FLI1–dependent repression of TGF-β receptor type 2, thereby sensitizing tumor cells to TGF-β ligands. Together, these findings suggest that Wnt/β-catenin–active tumor cells can contribute to Ewing sarcoma progression by promoting angiogenesis in the local TME.

Introduction

Tumor growth and metastatic progression are dependent on both tumor cell–autonomous factors and the local tumor microenvironment (TME) (1). Together, tumor cells and the TME, comprising secreted proteins, infiltrating nontumor stromal cells, blood vessels, and other structural and biochemical components, create an ecosystem conducive to tumor initiation and progression. In particular, creation of a supportive niche for tumor cells is heavily dependent on the composition and structure of the local extracellular matrix (ECM) (1). In addition, heterogeneity of tumor cells, the ECM, and other TME components, in time and space, contributes to a highly dynamic tumor ecosystem that modulates disease progression (2, 3).

Ewing sarcomas are aggressive bone and soft tissue tumors with peak incidence in adolescents and young adults (4). Pathologically, they are defined by an undifferentiated cellular histology and characteristic chromosomal translocations that create EWS-ETS fusion proteins, the most common of which is EWS-FLI1 (5). EWS-ETS fusions are critical for tumor initiation, maintenance, and progression and often represent the sole identifiable genetic lesion (6–8). However, although most primary Ewing sarcoma tumors harbor quiet genomes, the clinical outcomes differ widely among patients, among whom nearly a third ultimately succumb to disease recurrence and metastatic progression despite intensive multimodality therapy (4). To date, the mechanisms that contribute to disease progression remain poorly understood. Notably, however, cell-to-cell variability in levels of EWS-FLI1, and the inherent plasticity of Ewing sarcoma cells, contribute to tumor cell heterogeneity, and this heterogeneity has recently been implicated in the promotion of more aggressive disease (9–14). In addition, the critical contribution of nontumor stroma to clinical outcomes has also been reported (15). Thus, in order to advance understanding of the mechanisms that drive Ewing sarcoma relapse and metastasis, it is critical to elucidate the factors that contribute to the dynamic Ewing sarcoma ecosystem, in particular to heterogeneity of tumor cells and the TME.

Authorship note: AGH and EAP contributed equally to this work.

Conflict of interest: The authors have declared that no conflict of interest exists.

Submitted: November 21, 2019
Accepted: June 3, 2020
Published: July 9, 2020.

Reference information: *JCI Insight*. 2020;5(13):e135188. https://doi.org/10.1172/jci.insight.135188.

Canonical Wnt signaling is critical for normal development and is co-opted in cancer to promote proliferation, survival, and metastasis (16). In Ewing sarcoma, activating mutations in canonical Wnt signaling are uncommon, and only rare nuclear β-catenin–positive cells are present in tumor cell lines and patient biopsies (6–8, 11). Nevertheless, evidence of high Wnt/β-catenin activity is associated with worse clinical outcomes (11), suggesting that Wnt-activated tumor cells contribute to disease progression through mechanisms that have yet to be elucidated. We and others have shown that provision of exogenous canonical Wnt ligands can induce β-catenin/TCF signaling in discrete subpopulations of Ewing sarcoma cells, and these cells undergo a phenotypic switch to a more metastatic cell state (11, 17). Notably, these Wnt/β-catenin–induced cell state changes are associated with antagonism of EWS-ETS–dependent transcriptional activity (11, 18). Thus, Ewing sarcoma cells with active β-catenin/TCF signaling functionally mimic the more metastatic EWS-FLI1^{lo} state (9, 12). In addition, we recently reported that canonical Wnt pathway activation induces Ewing sarcoma cells to upregulate secretion of ECM proteins (19). In particular, Wnt/β-catenin–activated Ewing cells secrete collagens and matricellular proteins that contribute to tumor niches and promote local and metastatic tumor growth of other human cancers (20). This observation led us to test the hypothesis that, in addition to cell-autonomous changes, Wnt-activated Ewing sarcoma cells may influence tumor progression by altering the local TME. In the current study we report our potentially novel findings implicating Wnt/β-catenin–active tumor cell subpopulations in promotion of the angiogenic switch.

Results

Wnt/β-catenin activation in primary patient biopsies is associated with increased angiogenesis. Only rare subpopulations of Ewing tumor cells show evidence of canonical Wnt pathway activation in vivo, and high β-catenin transcriptional activity is associated with worse event-free and overall survival (11). These observations, together with our finding that Wnt/β-catenin–active tumor cells alter their secretomes (19), led us to hypothesize that Wnt/β-catenin–active cells may influence tumor progression by modulating the tumor microenvironment (TME). To address this hypothesis, we first evaluated whether expression of lymphoid enhancer binding factor 1 (*LEF1*), a previously established marker for activated Wnt/β-catenin in Ewing sarcoma tumor cells (11), in primary tumors correlates with expression of genes involved in tumor/TME interaction. We first identified genes that were highly positively correlated with *LEF1* (Pearson's $r > 0.5$) in 2 patient cohorts (15, 21). Gene ontology analysis of these independent gene sets revealed significant enrichment of biologic processes involved in ECM organization, cell adhesion, and angiogenesis (Figure 1, A and B). Subsequent unbiased analysis of these patient biopsy–derived data using gene set enrichment analysis (GSEA) confirmed statistically significant and reproducible correlations between *LEF1* and angiogenesis (Supplemental Figure 1A; supplemental material available online with this article; https://doi.org/10.1172/jci.insight.135188DS1). In addition, a direct and highly significant correlation was observed between *LEF1* and the endothelial cell–specific markers *CDH5* and *PECAM1* (Figure 1C). In contrast, *MYC* and *CCND1*, established targets of β-catenin in endothelial cells, did not correlate with *LEF1* in Ewing tumor biopsies (Figure 1D). Ewing sarcoma cells did not express either *CCH5* or *PECAM1*, and neither *MYC* nor *CCND1* were β-catenin/TCF target genes in this tumor (Supplemental Figure 1B and ref. 11). Thus, patient biopsies with transcriptional evidence of Wnt/β-catenin–active tumor cells displayed gene signatures that are consistent with enhanced endothelial cell infiltration and angiogenesis. In support of this, tumor biopsies with high fibrovascular stromal content expressed higher levels of *LEF1* than stroma-poor tumors (Supplemental Figure 1C and ref. 15). Moreover, there was a striking correlation between a stroma-associated prognostic gene signature and *LEF1* expression in patient biopsies (Figure 1, E and F), a signature that is highly enriched for genes involved in blood vessel development (15).

Together, these patient tumor data led us to investigate the hypothesis that Wnt/β-catenin–active Ewing sarcoma tumor cells influence angiogenesis in the local TME.

Canonical Wnt signaling in Ewing sarcoma cells contributes to the angiogenic switch in the local TME. Tumor angiogenesis is essential for tumor progression and requires sprouting of de novo blood vessels from vascular endothelial cells in the TME. This process is termed the angiogenic switch, and it is mediated by induction of a distinct transcriptional signature that is critically dependent on tumor/TME crosstalk (22–24). To determine whether there is a relationship between abundant Wnt/β-catenin–active tumor cells and the angiogenic switch in Ewing sarcoma, we first interrogated primary tumor data. Patient tumor signatures show a striking and reproducible enrichment of core angiogenic switch genes among *LEF1*-correlated transcripts (Figure 2A). To address whether angiogenic switch genes are induced by canonical Wnt signaling

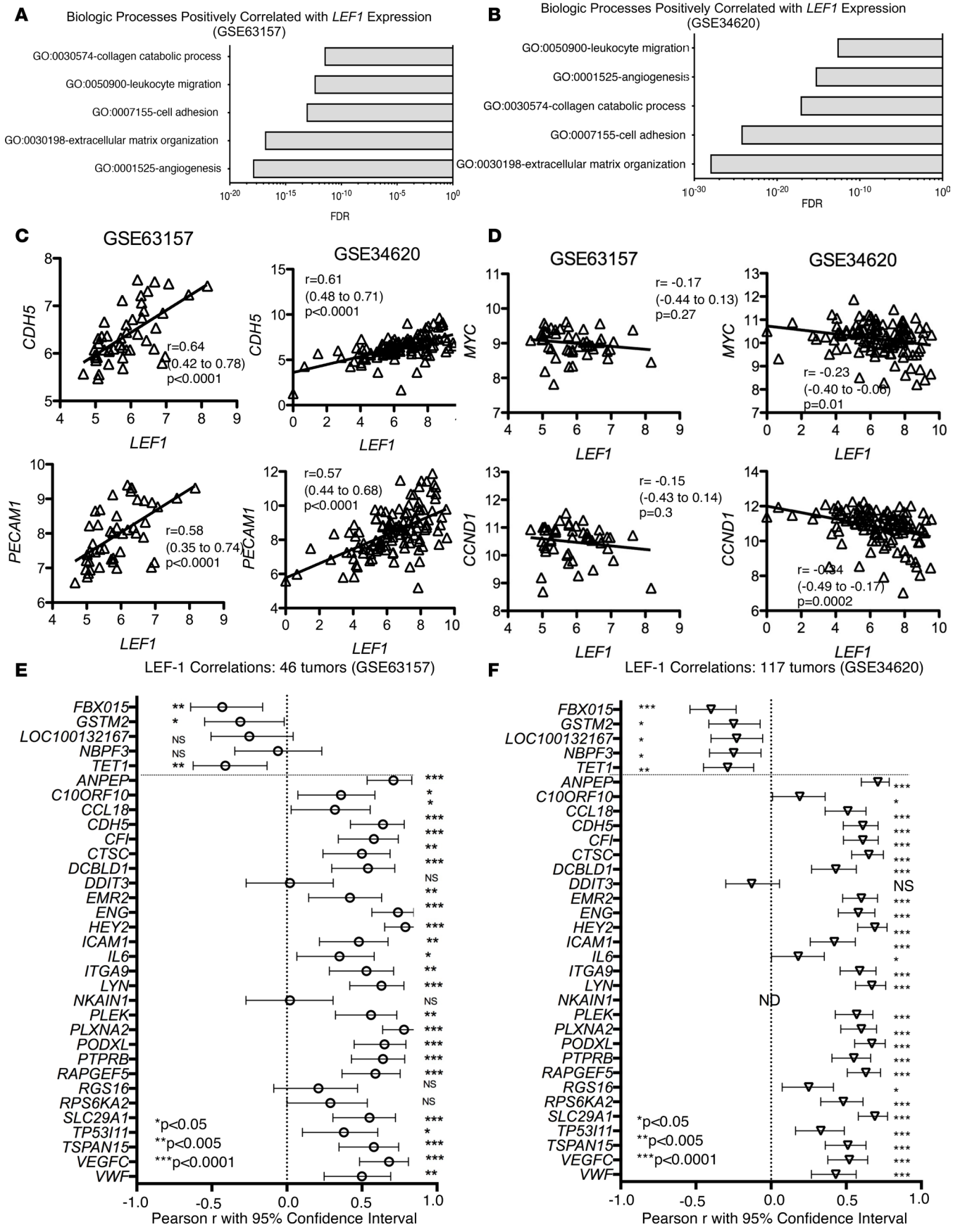
A
Biologic Processes Positively Correlated with LEF1 Expression (GSE63157)
GO:0030574-collagen catabolic process
GO:0050900-leukocyte migration
GO:0007155-cell adhesion
GO:0030198-extracellular matrix organization
GO:0001525-angiogenesis
FDR
B
Biologic Processes Positively Correlated with LEF1 Expression (GSE34620)
GO:0050900-leukocyte migration
GO:0001525-angiogenesis
GO:0030574-collagen catabolic process
GO:0007155-cell adhesion
GO:0030198-extracellular matrix organization
FDR
C
GSE63157
GSE34620
CDH5
r=0.64 (0.42 to 0.78) p<0.0001
r=0.61 (0.48 to 0.71) p<0.0001
PECAM1
r=0.58 (0.35 to 0.74) p<0.0001
r=0.57 (0.44 to 0.68) p<0.0001
LEF1
D
GSE63157
GSE34620
MYC
r= -0.17 (-0.44 to 0.13) p=0.27
r= -0.23 (-0.40 to -0.06) p=0.01
CCND1
r= -0.15 (-0.43 to 0.14) p=0.3
r= -0.34 (-0.49 to -0.17) p=0.0002
LEF1
E
LEF-1 Correlations: 46 tumors (GSE63157)
FBX015
GSTM2
LOC100132167
NBPF3
TET1
ANPEP
C10ORF10
CCL18
CDH5
CFI
CTSC
DCBLD1
DDIT3
EMR2
ENG
HEY2
ICAM1
IL6
ITGA9
LYN
NKAIN1
PLEK
PLXNA2
PODXL
PTPRB
RAPGEF5
RGS16
RPS6KA2
SLC29A1
TP53I11
TSPAN15
VEGFC
VWF
*p<0.05
**p<0.005
***p<0.0001
Pearson r with 95% Confidence Interval
F
LEF-1 Correlations: 117 tumors (GSE34620)
ND
Pearson r with 95% Confidence Interval

Figure 1. Wnt/β-catenin activation in primary patient biopsies is associated with increased angiogenesis. (**A** and **B**) Gene ontology analysis of *LEF1*-correlated genes ($r > 0.5$) was performed for 2 independent patient cohorts: GSE63157 ($N = 46$ Ewing tumors) and GSE34620 ($N = 117$ Ewing tumors). The top 5 most enriched biologic processes for each cohort are shown. GSE63157 ($N = 46$ Ewing tumors): ECM organization, 35 genes; cell adhesion, 46 genes; and angiogenesis, 38 genes. GSE34620 ($N = 117$ Ewing tumors): ECM organization, 57 genes; cell adhesion, 80 genes; and angiogenesis, 46 genes. For gene ontology (**A** and **B**), multiple test comparison was computed using FDR. Only gene sets with FDR < 0.05 are displayed. (**C**) Pearson's correlation (*r*) between *LEF1* and endothelial cell markers *CDH5* and *PECAM1* (with associated 95% CIs) in tumor biopsies. (**D**) Pearson's correlation (*r*) and 95% CI between *LEF1* and established target genes of Wnt/β-catenin in endothelial cells (*MYC*, *CCND1*). Gene expression data expressed as $\log_2$ signal intensity. (**E** and **F**) Pearson's correlations (*r*) of *LEF1* expression (error bars: 95% CIs) with 33 gene prognostic signatures in 2 independent patient cohorts. The first 5 genes were identified as good prognosis biomarkers whereas high expression of the remaining 28 genes (below horizontal dotted line) was associated with poor prognosis. NS, not significant; ND, no data available for indicated gene. Two-sided *t* tests were used to compute *P* values for **C**–**F**, and *P* values are shown for each gene. $^*P < 0.05$, $^{**}P < 0.005$, $^{***}P < 0.0001$.

in the tumor cells themselves, we compared expression of these genes in β-catenin/TCF–active and β-catenin/TCF–inactive tumor cells (GSE75859, ref. 11). Unsupervised hierarchical clustering of 289 angiogenic switch signature genes across 9 independent samples revealed overall heterogeneity of expression but segregated cells into 2 distinct clusters comprising β-catenin/TCF–active and β-catenin/TCF–inactive cells, respectively (Supplemental Figure 2). Evaluation of the intersection between all angiogenic switch genes and genes that were significantly differentially expressed by β-catenin/TCF–active cells identified 32 transcripts (31 unique genes), and all were upregulated in the context of canonical Wnt activation (overlap *P* value = $1.43e^{-4}$) (Figure 2, B and C). Thus, Ewing sarcomas with high levels of canonical Wnt activity have robust activation of the angiogenic switch gene signature, and expression of a significant proportion of these core angiogenesis-promoting genes is directly induced in the tumor cells themselves.

Having demonstrated a direct relationship between tumor cell–autonomous Wnt/β-catenin activation and induction of the angiogenic switch gene signature, we turned to established model systems to test whether β-catenin–activated tumor cells functionally affect angiogenesis in the TME. First, we tested function in vitro. Ewing sarcoma cells were engineered to stably express constitutively active β-catenin (EBP) as previously described (11), and upregulation of both *LEF1* and *AXIN2* was confirmed in these cells (Figure 3A). Conditioned medium (CM) from control and EBP cells was added to human umbilical vascular endothelial cells (HUVECs), and HUVEC proliferation and viability were measured over time (Figure 3B). As shown, proliferation (Figure 3C) and viability (Figure 3D) increased when HUVECs were exposed to EBP CM compared with control CM. The effect was observed as early as 24 hours after addition of the CM. Next, we used the chick chorioallantoic membrane (CAM) assay, a well-established model of tumor-induced angiogenesis that permits evaluation of the angiogenic switch in a physiologic TME in vivo (25). GFP^+ control and EBP cells were inoculated on CAMs, and tumor engraftment and vascularization were assessed after 72 hours (Figure 4, A–D). Both control and EBP cells reliably formed tumor nodules, and no difference in mass size was apparent at 3 days. However, significant differences in angiogenesis were detected. Specifically, in both A673 (Figure 4, A and B) and CHLA10 (Figure 4, C and D), activation of β-catenin in the tumor cells resulted in increased tumor vascularization. Thus, Ewing sarcoma cells can directly promote angiogenesis, and the capacity to induce endothelial cell proliferation and the angiogenic switch is enhanced when tumor cells express active β-catenin.

Wnt/β-catenin–activated tumor cells produce angiomatrix. Given our observation that CM from EBP Ewing sarcoma cells augments endothelial cell proliferation, we reasoned that induction of the angiogenic switch in the Ewing sarcoma TME is at least partially mediated by secreted factors that are derived from tumor cells. Secreted factors figure prominently among angiogenic switch genes, including proteins and cytokines that can be produced by stromal cells, tumor cells, or both (22, 23). In addition, over 100 ECM-encoding and ECM-associated protein–encoding genes were specifically identified as core angiogenic switch genes in the murine RIP-Tag angiogenic switch model (24). These 110 genes are highly enriched for matrisomal protein-encoding genes and have been collectively termed the angiomatrix (24). Notably, ECM-encoding genes were highly enriched among *LEF1*-correlated genes in Ewing tumor biopsies (Figure 1, A and B; and Supplemental Figure 3A), and GSEA revealed a striking and reproducible positive correlation between *LEF1* and the angiomatrix signature specifically (Figure 5A). To test whether angiomatrix genes and proteins are induced by Wnt/β-catenin signaling in tumor cells themselves, we compared the transcriptomes of β-catenin/TCF–active and β-catenin/TCF–inactive tumor cells, as described above. As shown, ECM-encoding genes were highly enriched among induced angiogenic switch genes (Supplemental Figure 3B), and β-catenin/TCF–active and –inactive cells segregated on the basis of

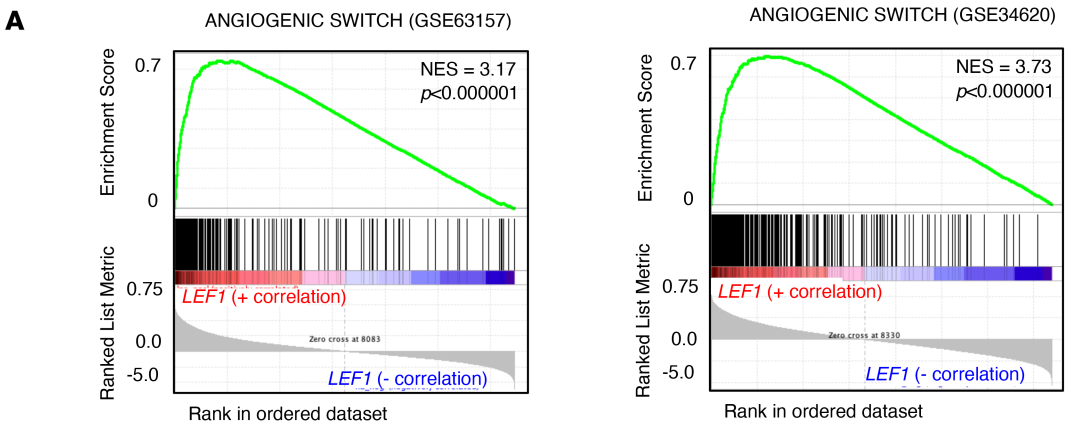

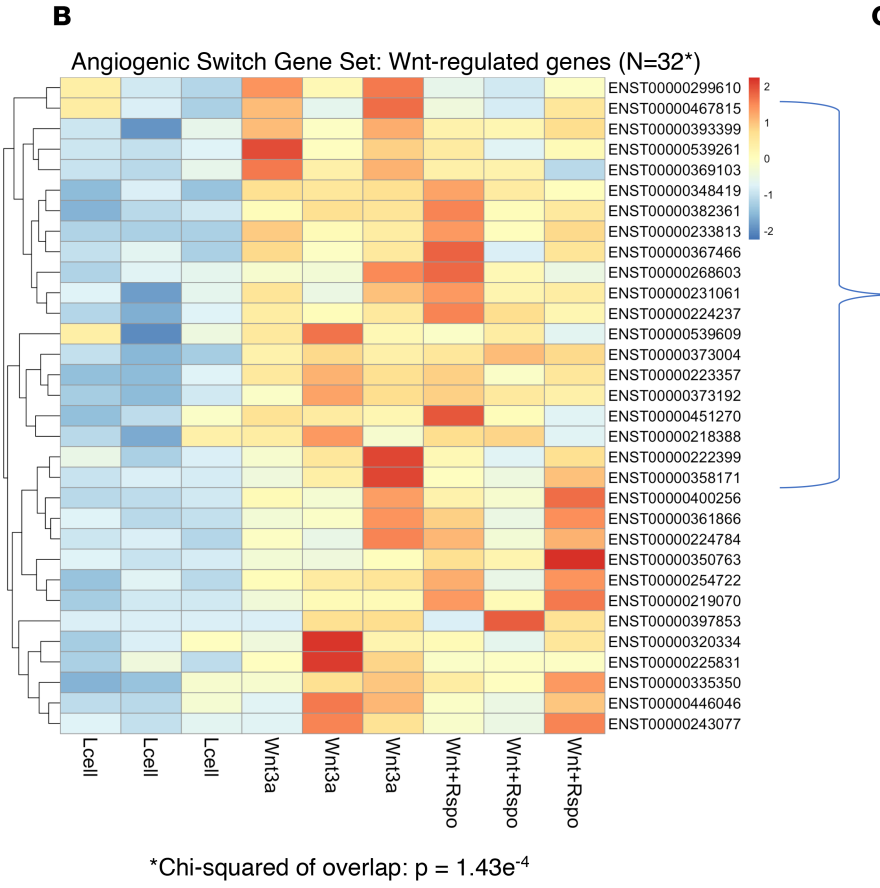

C

Ensembl Transcript ID	HGNC symbol
ENST00000299610	MFAP4
ENST00000467815	SULF2
ENST00000393399	PRCP
ENST00000539261	MGP
ENST00000369103	RGS10
ENST00000348419	CNN2
ENST00000382361	FSCN1
ENST00000233813	IGFBP5
ENST00000367466	PLA2G4A
ENST00000268603	CDH11
ENST00000231061	SPARC
ENST00000224237	VIM
ENST00000539609	ZEB2
ENST00000373004	SRPX2
ENST00000223357	AEBP1
ENST00000373192	UNC5B
ENST00000451270	ANXA2
ENST00000218388	TIMP1
ENST00000222399	LAMB1
ENST00000358171	SERPINH1
ENST00000400256	COLEC12
ENST00000361866	COL6A1
ENST00000224784	ACTA2
ENST00000350763	TNC
ENST00000254722	SERPINF1
ENST00000219070	MMP2
ENST00000397853	NDRG2
ENST00000320334	OLFML3
ENST00000225831	CCL2
ENST00000335350	UNC5B
ENST00000446046	FN1
ENST00000243077	LRP1

Figure 2. Wnt-activated Ewing sarcoma cells induce the angiogenic switch gene signature. (**A**) Unbiased GSEA of *LEF1*-correlated genes in 2 independent tumor cohorts as in Figure 1. All expressed transcripts were ranked on the basis of *LEF1* correlations, from positive to negative. For GSEA, 2-sided *t* tests were performed followed by multiple test comparison using FDR. Only gene sets with FDR < 0.05 are displayed. (**B**) Heatmap demonstrating relative expression of differentially expressed angiogenic switch genes in β-catenin/TCF–active cells compared with β-catenin/TCF–inactive cells. Data from ref. 11 (GSE75859) wherein CHLA25 Ewing sarcoma cells were treated with control or Wnt3a CM ± R-spondin 2 and β-catenin/TCF–active and –nonactive cells were isolated by FACS on the basis of TCF-GFP reporter activity. Data are expressed as fold change in expression in GFP^+ tumor cells compared with GFP^- control cells. (**C**) Corresponding official gene ID for ensembl transcripts represented in heatmap in **B**. *P* value for overlap between Wnt pathway–regulated genes and angiogenic switch genes was computed using χ^2 test.

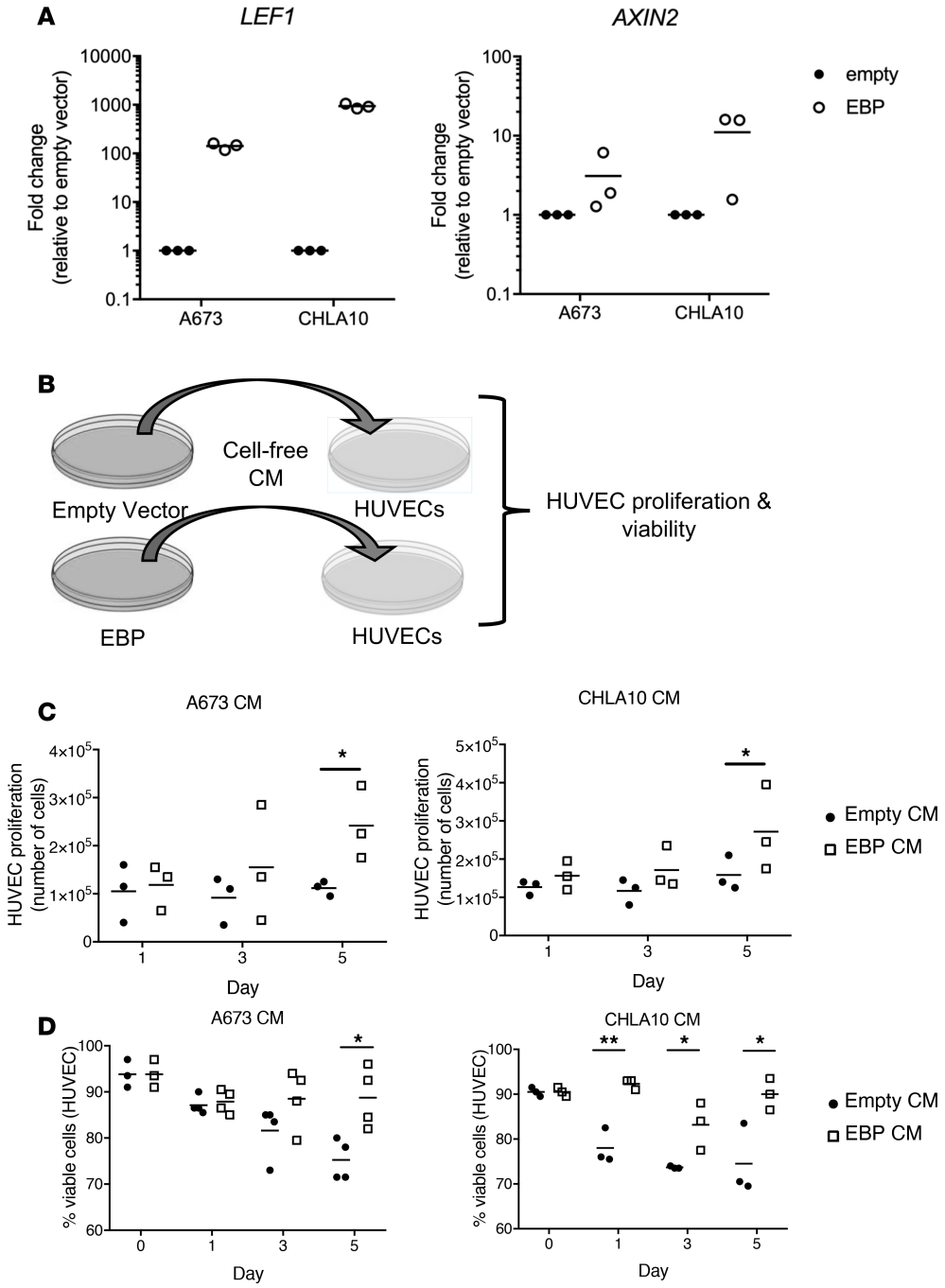

Figure 3. β-Catenin–activated Ewing cells secrete factors that promote HUVEC proliferation. (**A**) Expression of β-catenin target genes in A673 and CHLA10 cells following stable transduction with empty vector or constitutively active β-catenin (EBP). Levels were determined by quantitative real-time PCR (qRT-PCR) in each sample, and expression was normalized to housekeeping genes. Data shown are fold change relative to empty vector for 3 independent biologic replicates. (**B**) CM from A673 and CHLA10 cells containing either empty or EBP vector was collected and added to HUVECs. Proliferation (**C**) and viability (**D**) of HUVECs were measured 1, 3, and 5 days following addition of Ewing CM. *P* values were computed using 2-tailed *t* tests (**A**–**D**). $^*P < 0.05$, $^{**}P < 0.01$, $n \geq 3$ independent experiments (**A**–**D**).

angiomatrix gene expression (Supplemental Figure 3C). No angiomatrix genes were downregulated in β-catenin/TCF–active cells whereas 17 of 110 angiomatrix genes were significantly upregulated (overlap *P* value = $5.53e^{-5}$) (Figure 5, B and C). This induction of the angiomatrix gene signature is corroborated by analysis of Ewing sarcoma cell secretomes (19). Angiomatrix proteins were significantly overrepresented among those that we identified as being secreted by Wnt3a-exposed Ewing sarcoma cells (Figure 5D).

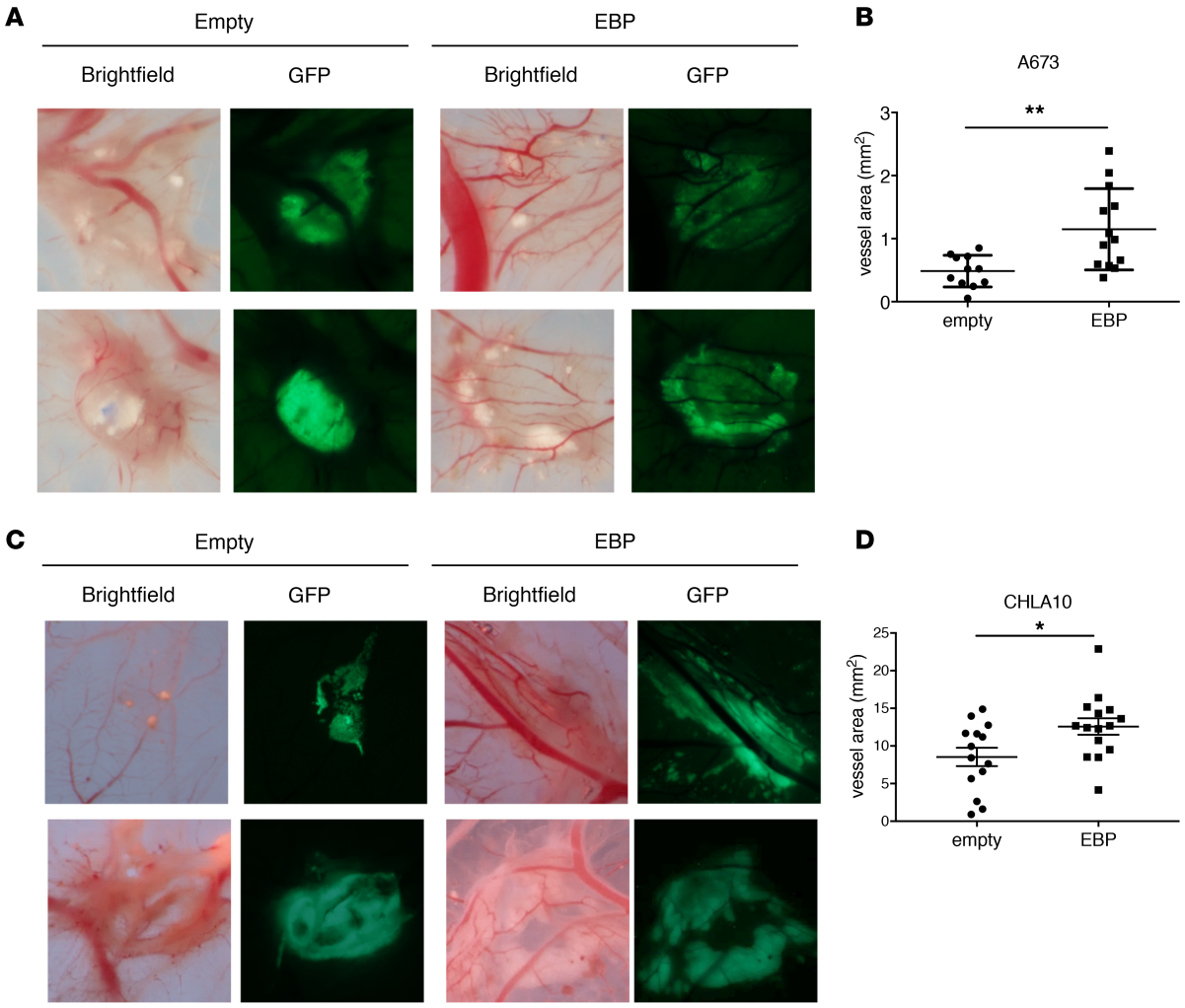

Figure 4. β-Catenin–activated Ewing sarcoma cells promote the angiogenic switch in vivo. (**A**–**D**) EBP and control cells were placed on the chick CAM for 72 hours. Tumors were located by GFP, and blood vessels were photographed under a stereoscope (**A** and **C**). Quantification of blood vessel area is shown for A673 (**B**) and CHLA10 (**D**). *P* values were computed using 2-tailed *t* tests (**B** and **D**). $^{*}P < 0.05$, $^{**}P < 0.01$, $n \geq 12$ independent experiments per condition (**B** and **D**).

Together these data demonstrate that, in response to canonical Wnt activation, Ewing sarcoma tumor cells upregulate transcription and secretion of angiomatrix proteins, and we propose that these proteins are likely to play a key role in promotion of the angiogenic switch.

Induction of the angiomatrix by Wnt/β-catenin–active tumor cells is dependent on TGF-β. Canonical Wnt target genes are highly dependent on cell context and cell type. Having identified a significant association between Wnt/β-catenin activation and the angiogenic switch in Ewing sarcoma, we next questioned whether induction of angiogenesis genes in tumor cells is mediated directly by β-catenin/TCF transcriptional complexes. Unexpectedly, we observed no enrichment of TCF binding sites in the promoters of genes that are differentially induced in β-catenin/TCF–active versus –inactive cells (Supplemental Table 1A), nor was there enrichment of TCF binding sites in *LEF1*-correlated angiogenic switch genes in primary tumors (Supplemental Table 1B). This led us to hypothesize that induction of the angiogenic switch in Ewing sarcoma cells may be an indirect rather than a direct effect of Wnt/β-catenin activation. In other cancers, the angiogenic switch is largely mediated by TGF-β signaling in nontumor stromal cells, and many angiomatrix genes are direct targets of SMAD transcriptional complexes (20, 24, 26). Early studies of Ewing sarcoma indicated that Ewing tumor cells are largely unresponsive to TGF-β ligands as a consequence of EWS-ETS–mediated repression of the TGF-β receptor type 2 (*TGFBR2*) locus (27). In agreement with this, we found that expression of *TGFBR2* is nearly undetectable in Ewing sarcoma cells and that knockdown of EWS-FLI1 results in robust induction of this receptor subunit (Figure 6, A and B). We previously discovered that many EWS-FLI1–repressed genes are induced by Wnt/β-catenin (11),

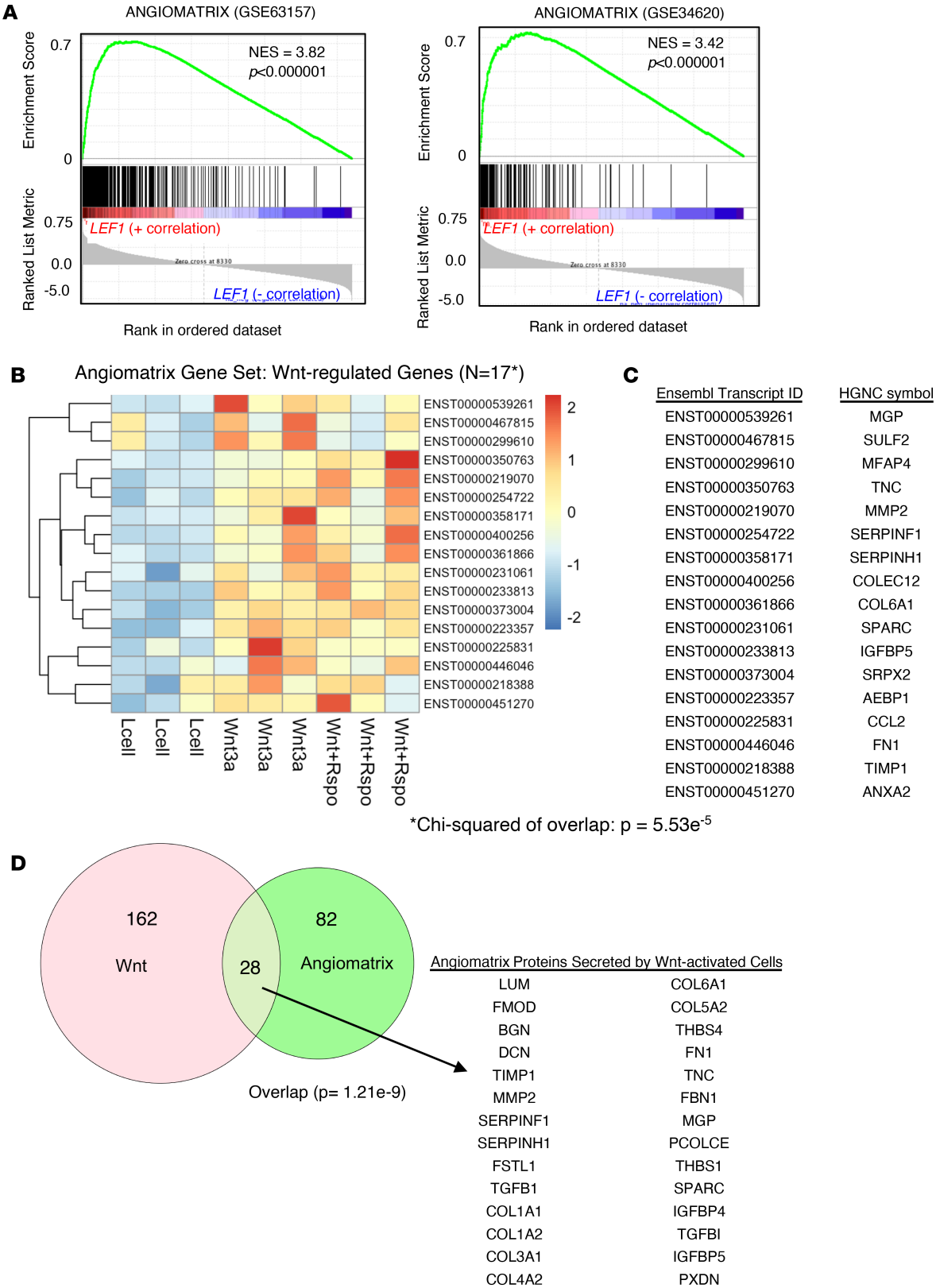

Figure 5. Wnt/β-catenin–activated tumor cells produce angiomatrix. (**A**) Unbiased GSEA of angiomatrix gene set among *LEF1*-correlated genes in 2 Ewing patient tumor cohorts as described in Figure 1. For GSEA, 2-sided *t* tests were performed followed by multiple test comparison using FDR. Only gene sets with FDR < 0.05 are displayed. (**B**) Heatmap demonstrating relative expression of differentially expressed angiomatrix genes in β-catenin/TCF–active cells compared with β-catenin/TCF–inactive cells as described in Figure 2. (**C**) Corresponding official gene ID for ensembl transcripts represented in heatmap in **B**. (**D**) Overlap between angiomatrix proteins and proteins secreted from Ewing sarcoma cells following canonical Wnt activation (TC32 secretome, *PXD007909*). List of the 28 overlapping proteins is shown. *P* values for overlaps were computed using χ^2 test.

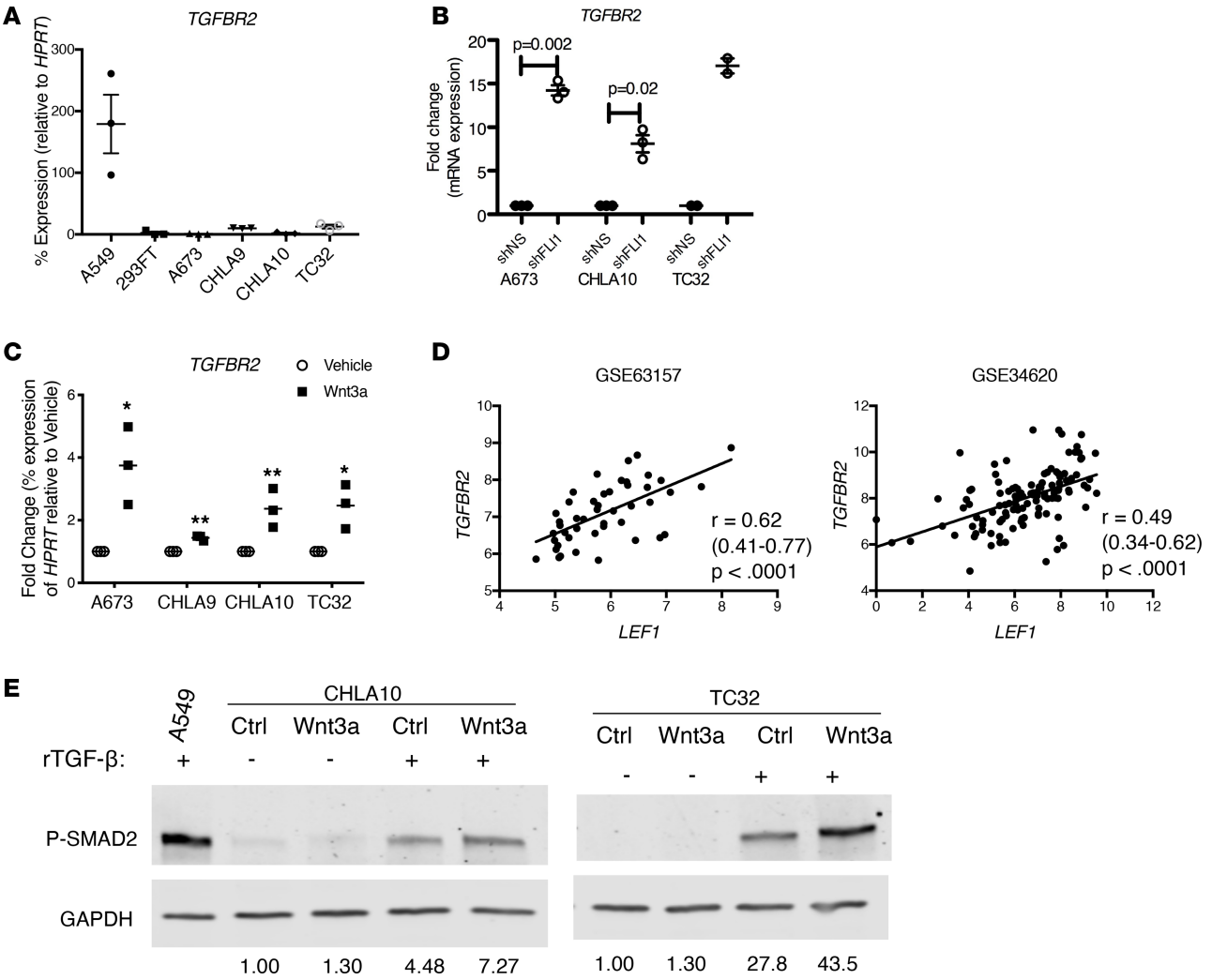

Figure 6. Wnt/β-catenin sensitizes Ewing sarcoma cells to TGF-β pathway activation. (**A**) qRT-PCR analysis of baseline *TGFBR2* expression in Ewing sarcoma (A673, CHLA9, CHLA10, TC32), embryonic kidney cells (293FT cells purchased from ATCC) (negative control), and lung adenocarcinoma (A549) cell lines (positive control) (N = 3 replicates per cell line). (**B**) Measurement of *TGFBR2* expression by qRT-PCR in Ewing sarcoma cells following knockdown of EWS-FLI1 (shFLI1). Expression is shown as fold change relative to cells transduced with nontargeting shRNA sequence (shNS). Results of replicate experiments are shown (N = 3, A673 and CHLA10; N = 2, TC32). P values were computed using 2-tailed t tests (**A**–**C**). $^*P < 0.05$, $^{**}P < 0.005$ (**A** and **C**). (**C**) qRT-PCR of *TGFBR2* expression in Ewing sarcoma cell lines following exposure to vehicle or recombinant Wnt3a (N = 3). (**D**) Correlation between *LEF1* and *TGFBR2* expression in patient tumor biopsies. GSE63157: N= 46 tumors; GSE34620: N = 117 tumors. Correlation was computed using Pearson's correlation, and P values were determined using 2-sided t tests. (**E**) Western blot analysis for phospho-SMAD2 (p-SMAD2) was performed on whole-cell lysates from CHLA10 and TC32 cells treated with control L cell (Ctrl) or Wnt3a CM (Wnt3a) ± TGFB1 for 1 hour. GAPDH served as the loading control and A549 as positive control for activated TGF-β signaling. Densitometry was used to calculate p-SMAD2 levels in each condition relative to Ctrl cells without TGFB1.

so we questioned whether *TGFBR2* may be derepressed under conditions of Wnt3a stimulation. Indeed, our studies showed that expression of *TGFBR2* was increased in Ewing sarcoma cells that were exposed to Wnt3a (Figure 6C). In addition, expression of *TGFBR2* directly correlated with *LEF1* in primary tumors, providing additional evidence that canonical Wnt signaling might influence the TGF-β response in Ewing sarcoma cells (Figure 6D). In support of this, pretreatment of Ewing sarcoma cells with Wnt3a CM augmented their sensitivity to TGF-β as evidenced by increased SMAD2 phosphorylation compared with cells that were exposed to TGF-β without Wnt3a preconditioning (Figure 6E).

Having established that Wnt sensitizes Ewing sarcoma cells to TGF-β signals, we next tested whether the Wnt-induced angiogenic response is mediated in whole or in part by TGF-β. To achieve this, we performed RNA-sequencing of Wnt3a-treated TC32 cells in the presence and absence of SB505124, a chemical inhibitor of TGFBR1, which is the dimerization partner of TGFBR2 (Supplemental Figure 4A). TC32 cells were chosen for this analysis given that they secrete TGF-β ligands (19), thereby removing the need

for provision of exogenous TGF-β and allowing for identification of tumor cell–autonomous crosstalk. Over 200 genes ($N = 204$) were induced by Wnt3a, and induction of 77 of these was inhibited by SB505124 (Supplemental Figure 4B and Supplemental Table 2). Significantly, these 77 Wnt-3a–induced and TGF-β–dependent targets were highly enriched for genes involved in ECM organization (Figure 7A), the angiogenic switch (Supplemental Figure 4, C–E), and the angiomatrix (Figure 7, B–D). Independent analysis of additional cell lines confirmed that induction and secretion of the angiomatrix protein tenascin C by Wnt3a is blocked by SB505124 (Figure 7, E and F). Thus, the Wnt-induced production of angiomatrix by Ewing sarcoma tumor cells is largely dependent on downstream activation of TGF-β signaling.

The TGF-β–mediated angiogenic response is augmented in the β-catenin/TCF–active tumor cell subpopulation. We previously showed that not all Ewing sarcoma cells respond equally to canonical Wnt ligands and that, for as yet undefined reasons, only discrete subpopulations induce β-catenin/TCF transcription in response to Wnt3a (11). Given this phenotypic heterogeneity, we hypothesized that tumor cells that respond to Wnt3a with activation of β-catenin/TCF transcription would be more susceptible to Wnt/TGF-β crosstalk than Wnt-nonresponsive, β-catenin/TCF–inactive cells. To test this, we exposed Ewing sarcoma TCF reporter cells to Wnt3a or vehicle control and then sorted cells into Wnt-responsive (GFP^+) and Wnt-nonresponsive (GFP^-) populations (Figure 8A). As shown, expression of *TGFBR2* was relatively higher in GFP^+ cells (Figure 8B). Moreover, these Wnt-responsive subpopulations showed increased activation of a SMAD binding element reporter (SBE-luciferase) when exposed to TGF-β, supporting their differential sensitivity to TGF-β signaling (Figure 8C). Finally, angiomatrix genes were more robustly induced in GFP^+ cells compared with GFP^- cells, despite equivalent exposure to both canonical Wnt and TGF-β ligands (Figure 8, D and E). Thus, Ewing sarcoma tumor cells that are selectively responsive to canonical Wnt pathway activation upregulate proangiogenic gene programs when they are exposed to TGF-β. These studies demonstrate a previously unappreciated role for subpopulations of Wnt/β-catenin–activated Ewing sarcoma tumor cells in promotion of the angiogenic switch.

Discussion

In this work we provide evidence that activation of canonical Wnt signaling in Ewing sarcoma tumor cells contributes to activation of the angiogenic switch in the local TME. Mechanistically, our data show that this is mediated by crosstalk between Wnt and TGF-β signaling pathways in Wnt-responsive tumor cell subpopulations and the influence of these cells on stromal ECM and endothelial cells. In particular, our findings reveal that functional cooperation between canonical Wnt and TGF-β signaling plays a key role in induction of the angiomatrix. Specifically, we demonstrate that Wnt-responsive Ewing cells upregulate expression of *TGFBR2*, priming them to respond to TGF-β ligands. In turn, TGF-β signaling promotes tumor cell–derived production of tenascin C and other proangiogenic ECM factors. Importantly, initial activation of the Wnt/β-catenin/TCF transcriptional axis in Ewing sarcoma is not tumor cell autonomous and requires provision of exogenous Wnt ligands (11, 28). We thus propose that this critical crosstalk between tumor cells and their local TME is particularly relevant in the context of a primary or metastatic bone tumor ecosystem where canonical Wnt and TGF-β ligands exist in abundance.

Induction of angiogenesis is a hallmark of cancer (29). The impact of Wnt signaling on physiologic and pathologic angiogenesis is well established, in particular in the context of endothelial cells, where activation of *LEF1* directly promotes cell proliferation and proangiogenic phenotypes (30, 31). In addition, canonical and noncanonical Wnt signaling can indirectly affect endothelial proliferation by altering secretion of proangiogenic factors, such as VEGFs, matrix metalloproteinases, and basic fibroblast growth factor, from tumor cells (32). Known regulators of angiogenesis in Ewing sarcoma include VEGF and insulin like growth factor (reviewed in ref. 33). To our knowledge, a role for Wnt/β-catenin–responsive tumor cells in modulation of Ewing sarcoma angiogenesis has not previously been reported. Our data show that Wnt-activated Ewing sarcoma cells upregulate expression of a core angiogenic switch–associated transcriptional signature. This is accompanied by altered secretion of numerous angiogenesis proteins. In particular, upon β-catenin activation, Ewing tumor cells increase secretion of multiple ECM proteins that comprise the angiomatrix. Angiomatrix proteins have been implicated in activation of the angiogenic switch in multiple experimental models (22–24, 34). Consistent with this, our experimental data show that Ewing sarcoma cells that express constitutively active β-catenin secrete factors that promote endothelial cell proliferation in vitro and angiogenesis in CAM assays in vivo. Furthermore, interrogation of primary tumor transcriptomes reveals a reproducible and highly significant correlation between canonical Wnt

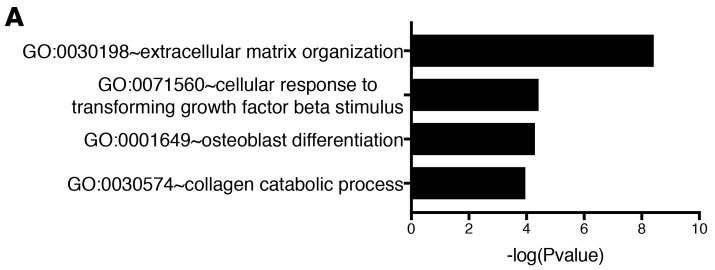

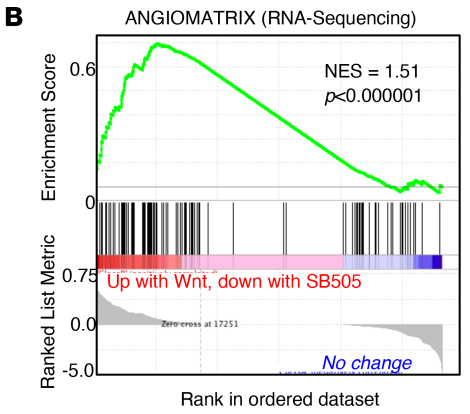

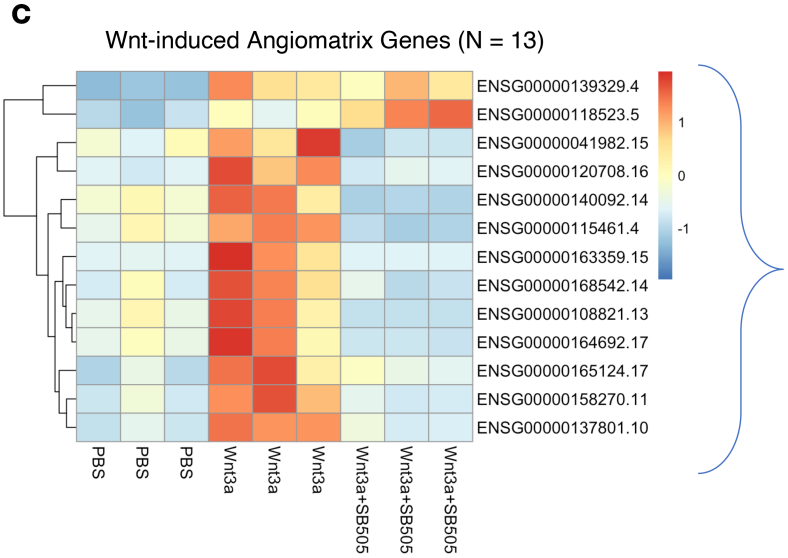

D

Wnt-induced/TGF-beta dependent angiomatrix Genes

Ensembl Transcript ID	HGNC symbol
ENSG00000139329.4	LUM
ENSG00000118523.5	CTGF
ENSG00000041982.15	TNC
ENSG00000120708.16	TGFBI
ENSG00000140092.14	FBLN5
ENSG00000115461.4	IGFBP5
ENSG00000163359.15	COL6A3
ENSG00000168542.14	COL3A1
ENSG00000108821.13	COL1A1
ENSG00000164692.17	COL1A2
ENSG00000165124.17	SVEP1
ENSG00000158270.11	COLEC12
ENSG00000137801.10	THBS1

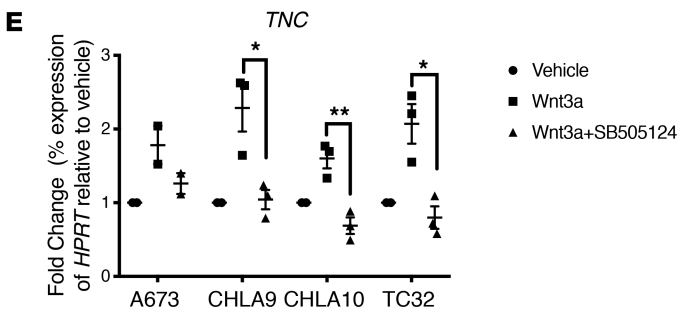

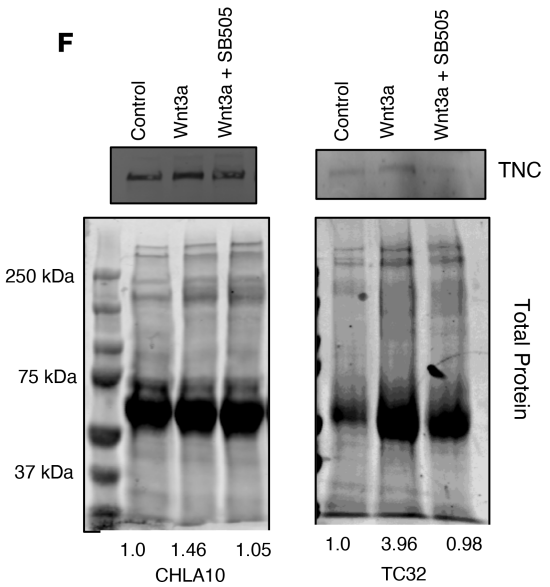

Figure 7. Induction of the angiomatrix by Wnt/β-catenin–active tumor cells is dependent on TGF-β. (**A**) Gene ontology (GO) of transcripts upregulated with Wnt3a and blocked by SB505124. Top 4 most enriched GO terms for biologic process are shown. (**B**) GSEA of transcripts ranked based on upregulation with Wnt and downregulation with SB505124 shows significant correlation with the angiomatrix (110 genes) gene signature. For GO and GSEA, multiple test comparison was computed using FDR. Only gene sets with FDR < 0.05 are displayed (**A** and **B**). (**C**) Heatmap showing relative expression levels of Wnt-induced angiomatrix genes following exposure to Wnt3a ± SB505124. (**D**) Corresponding official gene ID for ensembl transcripts represented in heatmap in **C**. Genes shown in red are Wnt3a-induced genes whose induction was blocked by TGF-β inhibition. (**E**) qRT-PCR of tenascin C (*TNC*) expression in Ewing sarcoma cell lines following exposure to vehicle or recombinant Wnt3a ± SB505124 (N = 3). P values were computed using 2-tailed t tests. $^*P < 0.05$, $^{**}P < 0.005$. (**F**) Secretion of TNC by Ewing sarcoma cells was measured by Western blot of CM after exposure to Wnt3a ± SB505124. Densitometry-based quantification was performed relative to total protein and compared with CM from unstimulated control cells.

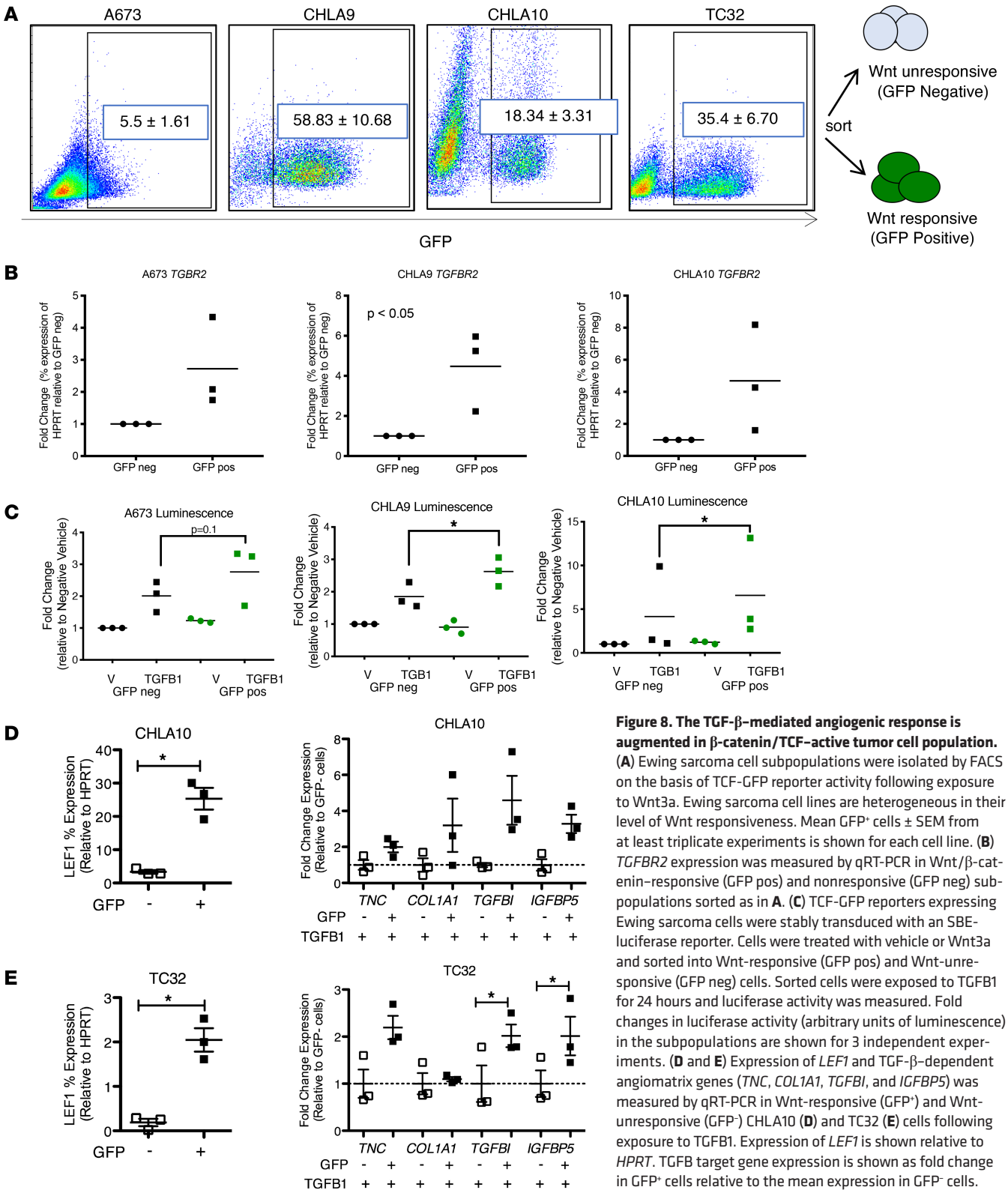

Figure 8. The TGF-β–mediated angiogenic response is augmented in β-catenin/TCF–active tumor cell population. (**A**) Ewing sarcoma cell subpopulations were isolated by FACS on the basis of TCF-GFP reporter activity following exposure to Wnt3a. Ewing sarcoma cell lines are heterogeneous in their level of Wnt responsiveness. Mean GFP⁺ cells ± SEM from at least triplicate experiments is shown for each cell line. (**B**) *TGFBR2* expression was measured by qRT-PCR in Wnt/β-catenin–responsive (GFP pos) and nonresponsive (GFP neg) subpopulations sorted as in **A**. (**C**) TCF-GFP reporters expressing Ewing sarcoma cells were stably transduced with an SBE-luciferase reporter. Cells were treated with vehicle or Wnt3a and sorted into Wnt-responsive (GFP pos) and Wnt-unresponsive (GFP neg) cells. Sorted cells were exposed to TGFB1 for 24 hours and luciferase activity was measured. Fold changes in luciferase activity (arbitrary units of luminescence) in the subpopulations are shown for 3 independent experiments. (**D** and **E**) Expression of *LEF1* and TGF-β–dependent angiomatrix genes (*TNC*, *COL1A1*, *TGFBI*, and *IGFBP5*) was measured by qRT-PCR in Wnt-responsive (GFP⁺) and Wnt-unresponsive (GFP⁻) CHLA10 (**D**) and TC32 (**E**) cells following exposure to TGFB1. Expression of *LEF1* is shown relative to *HPRT*. TGFB target gene expression is shown as fold change in GFP⁺ cells relative to the mean expression in GFP⁻ cells. *P* values were determined using 2-tailed paired *t* test in 3 independent sorting experiments, $^*P < 0.05$ (**B**–**E**).

activation and the angiogenic switch and angiomatrix signatures in patient tumors in vivo. Activation of the angiogenic switch can occur at multiple stages of tumor progression: it is essential for successful expansion of both primary and metastatic tumors, it is required for successful colonization of tumor cells as they establish new foci at distant sites, and it is implicated in conversion of premalignant and dormant cells to a malignant and active state (23). As such, tumors that are able to robustly activate the switch are generally more aggressive and are associated with worse clinical outcomes (22–24). Although clinically useful prognostic gene signatures have yet to be defined for Ewing sarcoma, we previously demonstrated that tumor interaction with the TME is a key determinant of poor prognosis in patients with localized disease (15). Importantly, we now show that a striking and reproducible correlation exists between expression of this poor prognosis gene signature, *LEF1*, and angiogenesis.

Given these data, we propose that disabling canonical Wnt signaling would be expected to inhibit the angiogenic switch, prevent Ewing sarcoma progression, and improve clinical outcomes. Therapeutic targeting of the Wnt/β-catenin axis remains a clinical challenge because of the difficulties inherent in targeting transcriptional networks and the high incidence of on-target side effects, which largely affect bone (35, 36). Nevertheless, there is precedent that targeting angiogenesis in these tumors is a worthy endeavor. Preclinical studies of VEGF inhibitors, such as bevacizumab, showed efficacy in preclinical models and clinical studies with combination approaches continue to be investigated (33). More recently, antibody-drug conjugates targeting the proangiogenic membrane receptor protein endoglin (ENG) have shown preclinical efficacy in Ewing models (37). ENG is highly expressed by endothelial cells, and by some Ewing tumor cells, and has been implicated in mediating tumor cell plasticity and invasion (38). Of note, *ENG* is a member of the angiogenic switch signature, is highly correlated with *LEF1* in primary tumors, and is identified as a poor prognosis gene marker in TME-rich tumor biopsies (Figure 1, E and F). In addition, the angiomatrix protein tenascin C is a known mediator of the angiogenic switch and metastatic progression (24, 39) and is of great interest as a therapeutic target (40). Our data now support that tenascin C is a robust downstream target of the Wnt/TGF-β–mediated angiogenic response in Ewing sarcoma tumor cells. Thus, in Ewing sarcoma, canonical Wnt signaling cooperates with TGF-β to activate the angiogenic switch in the Wnt/β-catenin–active tumor cell compartment. We propose that, given its role as an upstream regulator of such a critical and broad proangiogenic program, the Wnt/β-catenin axis deserves exploration as a target for adjuvant antiangiogenic therapeutics. Intriguingly, Tegavivint, a new β-catenin inhibitor, was recently reported to inhibit metastasis of osteosarcoma in preclinical models (41). We propose that further study of Wnt/β-catenin inhibition is warranted in the context of Ewing sarcoma, in particular for patients who are at high risk of relapse and metastatic progression.

Methods

Cell culture and reagents. Ewing sarcoma cell lines were obtained from the Children's Oncology Group (COG) cell bank (https://www.cccells.org), and identities of the cells were verified by short tandem repeat profiling. A673 and TC32 cells were cultured in RPMI 1640 medium (Life Technologies, Thermo Fisher Scientific) supplemented with 10% fetal bovine serum (FBS) (Atlas Biologicals) and 2 mM L-glutamine (Life Technologies, Thermo Fisher Scientific). CHLA9 and CHLA10 cells were cultured in IMDM (Life Technologies, Thermo Fisher Scientific), 20% FBS, 2 mM L-glutamine, and 1× insulin-transferrin-selenium supplement (Gibco, Thermo Fisher Scientific). Cells were maintained at a low passage for all experiments. Cells were routinely tested for mycoplasma. HUVECs were purchased from Lonza and cultured in medium 200 with low serum growth supplement (LSGS) (Thermo Fisher Scientific). GFP-tagged cells expressing a constitutively active β-catenin construct (EBP) or corresponding empty vector control were generated as previously described (11). To activate canonical Wnt signaling, cells were treated with either recombinant human Wnt3a (R&D Systems, Bio-Techne, 5036-WN) at a concentration of 100 ng/mL or Wnt3a CM collected from Wnt3a L cells (ATCC CRL-2647) (control: L cell CM from L cells, ATCC CRL-2648). To activate TGF-β signaling, cells were treated with recombinant human TGF-β1 (TGFB1) (R&D Systems, Bio-Techne, 240-B) at a concentration of 10 ng/mL. To inhibit the TGF-β signaling pathway, cells were treated with 10 μM ALK inhibitor SB-505124 (Cayman Chemical, 694433-59-5).

Clinical correlations. Expression data were extracted from previously published Ewing sarcoma data sets from COG (GSE63157) (15) and European collaborative studies (GSE34620) (21). Correlations were measured by Pearson's correlation and 95% CIs determined. GO analysis was performed using Database for Annotation, Visualization and Integrated Discovery (DAVID) (42).

Gene set enrichment analysis. An in vivo signature of Wnt/β-catenin signaling was generated by ranking genes based on correlation with *LEF1*, and GSEA was performed using the GseaPreranked function of GSEA v2.1.0 software (Broad Institute) (43). GO enrichment was determined using the same list of genes with a cutoff of Pearson's $r > 0.5$ and interrogated using DAVID v6.8 (42).

Motif analysis. Promoter regions of genes of interest were searched within 2 kb of their transcription start sites for enriched motifs. The findMotifs.pl function from the HOMER analysis suite was used to search for motifs of 8, 10, or 12 nucleotides in length (44).

Western blotting. Western blot analysis of secreted tenascin C was performed as previously described (19). For p-SMAD2 blots, cells were washed once with 1× phosphate-buffered saline (PBS; Gibco, Thermo Fisher Scientific) and then lysed in RIPA buffer (Thermo Fisher Scientific) containing 1× Complete Protease Inhibitor Cocktail and 1× PhosSTOP Phosphatase Inhibitor Cocktail (Roche) for 10 minutes at 4°C. Cell lysates were clarified by centrifugation at 16,000 *g* for 5 minutes at 4°C. Protein concentration was measured using the DC Protein Assay (Bio-Rad), and samples were resolved by 4-15% SDS-PAGE gels (Bio-Rad). Proteins were transferred onto nitrocellulose membranes and subjected to standard immunoblotting. Western blots were imaged and densitometry performed using the LI-COR Biosciences imaging system and software. Western blot antibodies included p-SMAD2 (Cell Signaling Technology, 3101, 1:1000), GAPDH (Invitrogen, Thermo Fisher Scientific, AM4300, 1:20,000), goat anti-rabbit IgG IRDye 800 (LI-COR Biosciences, 1:10,000), and goat anti-mouse IgG IRDye 680 (LI-COR Biosciences, 1:15,000).

Cell sorting and reporter studies. Ewing sarcoma cells stably transduced with a TCF/LEF-GFP reporter as previously described (11) were transduced with a lentiviral SBE-luciferin reporter with Cignal Lenti SMAD Reporter (luc) Kit (CLS-017L, QIAGEN). Cells were sorted using the MoFlo Astrios instrument (University of Michigan Flow Cytometry Core) on the basis of GFP expression posttreatment with recombinant Wnt3a for 48 hours. After sorting, cells were treated with vehicle (4 mM HCl in PBS) or TGFB1 for 24 hours before measuring luminescence or measuring gene expression via qRT-PCR. Luminescence was determined using the Pierce Firefly Luciferase Glow Assay Kit (Thermo Fisher Scientific, 16176). For qRT-PCR studies, GFP^- cells were replated in L cell CM, and GFP^+ cells were replated in Wnt3a CM after sorting.

EWS-FLI1 knockdown experiments. For knockdown experiments, the lentiviral pLKO.1 nontargeting shRNA (SHC002) and the shRNA for FLI1 (TRCN0000005322) were obtained from MilliporeSigma. Cells were transduced with lentivirus in complete medium, and 24 hours later medium was replaced. Forty-eight hours posttransduction, cells were selected using puromycin (1.5–2 μg/mL) for 48 hours (96 hours posttransduction) and collected.

RNA-sequencing analysis and gene expression analysis. TC32 cells were treated with vehicle (PBS) or Wnt3a (100 ng/mL) for 4 hours before treatment with DMSO or SB505124 (10 μM) for 24 hours. RNA was collected for each condition in triplicate, and single-end sequencing was done on the Illumina HiSeq 4000 (University of Michigan Sequencing Core). Quality control was assessed with MultiQC, and reads were aligned using STAR. Differential expression was determined with DESeq2. Genes with adjusted $P < 0.1$ and log(fold change) > 0.6 (Wnt + DMSO vs. vehicle) and log(fold change) < –0.6 (Wnt + DMSO vs. Wnt + SB505124) were used for further analysis (Supplemental Table 2). RNA-sequencing data have been deposited to GEO (GSE124523). GO analysis was performed using DAVID (42). GSEA was performed using the GseaPreranked function of GSEA v2.1.0 software (Broad Institute) (43). qRT-PCR was used to measure and compare gene expression between experimental conditions. Primer sequences are shown in Supplemental Table 3.

Chick CAM assay. Fertilized eggs were obtained from the Michigan State University Department of Animal Science poultry farm. Upon arrival, eggs were placed in a humidified, rocking incubator (GQF Manufacturing) at 37°C for 11 days (E11). On E11, eggs were assessed for viability of the embryo using a handheld light source (GQF Manufacturing). Eggs containing nonviable embryos were discarded. The CAM was "dropped" as previously described (25, 31), and 1×10^6 GFP-labeled A673 or CHLA10 cells were placed on the CAM in 2.5% growth factor–reduced Matrigel (BD Biosciences) in PBS. Cells were incubated for 3 days without rocking. On E14, the CAM was dissected out and fixed. Tumors on the CAM were identified and imaged by GFP fluorescence and bright-field microscopy on an Olympus SZX16 stereo dissecting macroscope and analyzed using NIS-Elements imaging software (Nikon). Vessel area within each GFP-defined tumor was quantified using ImageJ (NIH), specifically by removing the background using the "subtract background" function, thresholding the image on red pixels, and subsequently measuring the number of red pixels followed by conversion of pixel area to square millimeters.

HUVEC proliferation and viability assays. CM from EBP and control Ewing sarcoma cells was generated by plating 5×10^6 CHLA10 or 10×10^6 A673 cells on 10-cm dishes. Once adherent, cells were serum starved for 24 hours, and serum-free CM was aspirated and centrifuged at 900 rcf for 5 minutes to remove cell debris. CM was added in a 50:50 concentration to HUVECs plated at a density of 7.5×10^4 cells per well on 6-well plates, in M200 containing 0.25× LSGS. On days 1, 3, and 5, cells were dissociated with Accutase (Corning) and stained with trypan blue (Invitrogen, Thermo Fisher Scientific) before counting. Cell number and viability were determined using a Countess automated cell counter and confirmed manually on a hemocytometer.

Statistics. For all gene expression analysis, 2-tailed *t* tests were performed and *P* values were computed. For all analysis in which more than 2 comparisons were made, adjusted *P* values were computed. For RNA-sequencing analysis, adjusted *P* values were computed using the Benjamini-Hochberg method. For GO and GSEA, multiple test comparison was computed using FDR. Only gene sets with FDR < 0.05 are displayed. Correlations were measured by Pearson's correlation and 95% CIs determined. Comparisons were considered statistically significant at $P < 0.05$. Statistical significance of overlaps was determined using χ^2 goodness-of-fit test. All error bars represent mean ± SEM.

Study approval. All primary tumor data were obtained from publicly anonymized databases in accordance with Institutional Review Board approval.

Author contributions

AGH, EAP, and ERL designed and directed the project. ST, KT, CS, and JAR performed experiments. BM and AGH performed bioinformatics analysis. AGH, EAP, and ERL wrote the manuscript. ST, KT, CS, JAR, BM, RC, AGH, EAP, and ERL discussed the results and edited the final manuscript. Co–first authors are listed alphabetically.

Acknowledgments

This work was supported by the following grants: Rosa and Francesco Romanello St. Baldrick's Research Grant (ERL); SARC Sarcoma SPORE U54 CA168512 (ERL, RC); Cancer Biology Training Grant T32 CA009676, Advanced Proteome Informatics of Cancer T32 CA140044, and F99/K00 Predoctoral to Postdoctoral Transition Fellowship F99 CA234810 (AGH); NRSA F30 CA183276 (EAP); and P30CA046592 to the Rogel Cancer Center at the University of Michigan through use of the following shared resources: Biostatistics, Analytics and Bioinformatics; Cell and Tissue Imaging; Flow Cytometry; Immune Monitoring; and Tissue and Molecular Pathology. The authors also gratefully acknowledge additional funding support from the UM Pioneer Fellowship (KT), U Can-Cer Vive Foundation (ERL), and Russell G. Adderley endowment from the Department of Pediatrics.

Address correspondence to: Elizabeth R. Lawlor, 1100 Olive Way, Suite 100, Seattle, Washington 98101, USA. Phone: 206.884.0198; Email: beth.lawlor@seattle.childrens.org.

1. Quail DF, Joyce JA. Microenvironmental regulation of tumor progression and metastasis. *Nat Med*. 2013;19(11):1423–1437.
2. Meacham CE, Morrison SJ. Tumour heterogeneity and cancer cell plasticity. *Nature*. 2013;501(7467):328–337.
3. Caswell DR, Swanton C. The role of tumour heterogeneity and clonal cooperativity in metastasis, immune evasion and clinical outcome. *BMC Med*. 2017;15(1):133.
4. Balamuth NJ, Womer RB. Ewing's sarcoma. *Lancet Oncol*. 2010;11(2):184–192.
5. Lawlor ER, Sorensen PH. Twenty years on: what do we really know about Ewing sarcoma and what is the path forward? *Crit Rev Oncog*. 2015;20(3-4):155–171.
6. Brohl AS, et al. The genomic landscape of the Ewing Sarcoma family of tumors reveals recurrent STAG2 mutation. *PLoS Genet*. 2014;10(7):e1004475.
7. Crompton BD, et al. The genomic landscape of pediatric Ewing sarcoma. *Cancer Discov*. 2014;4(11):1326–1341.
8. Tirode F, et al. Genomic landscape of Ewing sarcoma defines an aggressive subtype with co-association of STAG2 and TP53 mutations. *Cancer Discov*. 2014;4(11):1342–1353.
9. Chaturvedi A, Hoffman LM, Welm AL, Lessnick SL, Beckerle MC. The EWS/FLI oncogene drives changes in cellular morphology, adhesion, and migration in Ewing sarcoma. *Genes Cancer*. 2012;3(2):102–116.
10. Wiles ET, Bell R, Thomas D, Beckerle M, Lessnick SL. ZEB2 represses the epithelial phenotype and facilitates metastasis in Ewing sarcoma. *Genes Cancer*. 2013;4(11-12):486–500.
11. Pedersen EA, et al. Activation of Wnt/β-catenin in Ewing sarcoma cells antagonizes EWS/ETS function and promotes phenotypic transition to more metastatic cell states. *Cancer Res*. 2016;76(17):5040–5053.
12. Franzetti GA, et al. Cell-to-cell heterogeneity of EWSR1-FLI1 activity determines proliferation/migration choices in Ewing sarcoma cells. *Oncogene*. 2017;36(25):3505–3514.

13. El-Naggar AM, et al. Translational activation of HIF1α by YB-1 promotes sarcoma metastasis. *Cancer Cell*. 2015;27(5):682–697.
14. Bailey KM, Airik M, Krook MA, Pedersen EA, Lawlor ER. Micro-environmental stress induces Src-dependent activation of invadopodia and cell migration in Ewing sarcoma. *Neoplasia*. 2016;18(8):480–488.
15. Volchenboum SL, et al. Gene expression profiling of Ewing sarcoma tumors reveals the prognostic importance of tumor-stromal interactions: a report from the Children's Oncology Group. *J Pathol Clin Res*. 2015;1(2):83–94.
16. Clevers H, Nusse R. Wnt/β-catenin signaling and disease. *Cell*. 2012;149(6):1192–1205.
17. Uren A, Wolf V, Sun YF, Azari A, Rubin JS, Toretsky JA. Wnt/Frizzled signaling in Ewing sarcoma. *Pediatr Blood Cancer*. 2004;43(3):243–249.
18. Navarro D, Agra N, Pestaña A, Alonso J, González-Sancho JM. The EWS/FLI1 oncogenic protein inhibits expression of the Wnt inhibitor DICKKOPF-1 gene and antagonizes beta-catenin/TCF-mediated transcription. *Carcinogenesis*. 2010;31(3):394–401.
19. Hawkins AG, et al. The Ewing sarcoma secretome and its response to activation of Wnt/beta-catenin signaling. *Mol Cell Proteomics*. 2018;17(5):901–912.
20. Lu P, Weaver VM, Werb Z. The extracellular matrix: a dynamic niche in cancer progression. *J Cell Biol*. 2012;196(4):395–406.
21. Postel-Vinay S, et al. Common variants near TARDBP and EGR2 are associated with susceptibility to Ewing sarcoma. *Nat Genet*. 2012;44(3):323–327.
22. Baeriswyl V, Christofori G. The angiogenic switch in carcinogenesis. *Semin Cancer Biol*. 2009;19(5):329–337.
23. Bergers G, Benjamin LE. Tumorigenesis and the angiogenic switch. *Nat Rev Cancer*. 2003;3(6):401–410.
24. Langlois B, et al. AngioMatrix, a signature of the tumor angiogenic switch-specific matrisome, correlates with poor prognosis for glioma and colorectal cancer patients. *Oncotarget*. 2014;5(21):10529–10545.
25. Kunzi-Rapp K, Genze F, Küfer R, Reich E, Hautmann RE, Gschwend JE. Chorioallantoic membrane assay: vascularized 3-dimensional cell culture system for human prostate cancer cells as an animal substitute model. *J Urol*. 2001;166(4):1502–1507.
26. Roberts AB, McCune BK, Sporn MB. TGF-beta: regulation of extracellular matrix. *Kidney Int*. 1992;41(3):557–559.
27. Hahm KB, et al. Repression of the gene encoding the TGF-beta type II receptor is a major target of the EWS-FLI1 oncoprotein. *Nat Genet*. 1999;23(2):222–227.
28. Scannell CA, et al. LGR5 is expressed by Ewing sarcoma and potentiates Wnt/β-catenin signaling. *Front Oncol*. 2013;3:81.
29. Hanahan D, Weinberg RA. Hallmarks of cancer: the next generation. *Cell*. 2011;144(5):646–674.
30. Olsen JJ, et al. The role of Wnt signalling in angiogenesis. *Clin Biochem Rev*. 2017;38(3):131–142.
31. Dejana E. The role of wnt signaling in physiological and pathological angiogenesis. *Circ Res*. 2010;107(8):943–952.
32. Zhang X, Gaspard JP, Chung DC. Regulation of vascular endothelial growth factor by the Wnt and K-ras pathways in colonic neoplasia. *Cancer Res*. 2001;61(16):6050–6054.
33. DuBois SG, Marina N, Glade-Bender J. Angiogenesis and vascular targeting in Ewing sarcoma: a review of preclinical and clinical data. *Cancer*. 2010;116(3):749–757.
34. Fang J, et al. Matrix metalloproteinase-2 is required for the switch to the angiogenic phenotype in a tumor model. *Proc Natl Acad Sci U S A*. 2000;97(8):3884–3889.
35. Danieau G, Morice S, Rédini F, Verrecchia F, Royer BB. New insights about the Wnt/β-catenin signaling pathway in primary bone tumors and their microenvironment: a promising target to develop therapeutic strategies? *Int J Mol Sci*. 2019;20(15):E3751.
36. Nusse R, Clevers H. Wnt/β-catenin signaling, disease, and emerging therapeutic modalities. *Cell*. 2017;169(6):985–999.
37. Puerto-Camacho P, et al. Preclinical efficacy of endoglin-targeting antibody-drug conjugates for the treatment of Ewing sarcoma. *Clin Cancer Res*. 2019;25(7):2228–2240.
38. Pardali E, et al. Critical role of endoglin in tumor cell plasticity of Ewing sarcoma and melanoma. *Oncogene*. 2011;30(3):334–345.
39. Oskarsson T, et al. Breast cancer cells produce tenascin C as a metastatic niche component to colonize the lungs. *Nat Med*. 2011;17(7):867–874.
40. Midwood KS, Chiquet M, Tucker RP, Orend G. Tenascin-C at a glance. *J Cell Sci*. 2016;129(23):4321–4327.
41. Nomura M, et al. Tegavivint and the β-Catenin/ALDH axis in chemotherapy-resistant and metastatic osteosarcoma. *J Natl Cancer Inst*. 2019;111(11):1216–1227.
42. Huang da W, Sherman BT, Lempicki RA. Systematic and integrative analysis of large gene lists using DAVID bioinformatics resources. *Nat Protoc*. 2009;4(1):44–57.
43. Subramanian A, et al. Gene set enrichment analysis: a knowledge-based approach for interpreting genome-wide expression profiles. *Proc Natl Acad Sci U S A*. 2005;102(43):15545–15550.
44. Heinz S, et al. Simple combinations of lineage-determining transcription factors prime cis-regulatory elements required for macrophage and B cell identities. *Mol Cell*. 2010;38(4):576–589.